The Mechanism of Platelet-Rich Plasma Added to Skin Flap Postoperative for the Influence of Skin Flap Survival

Authors

Chengyang Dong, Zean Lin, Linsen Fang

Correspondence

shaoshangke@126.com (L. Fang)

Graphical Abstract

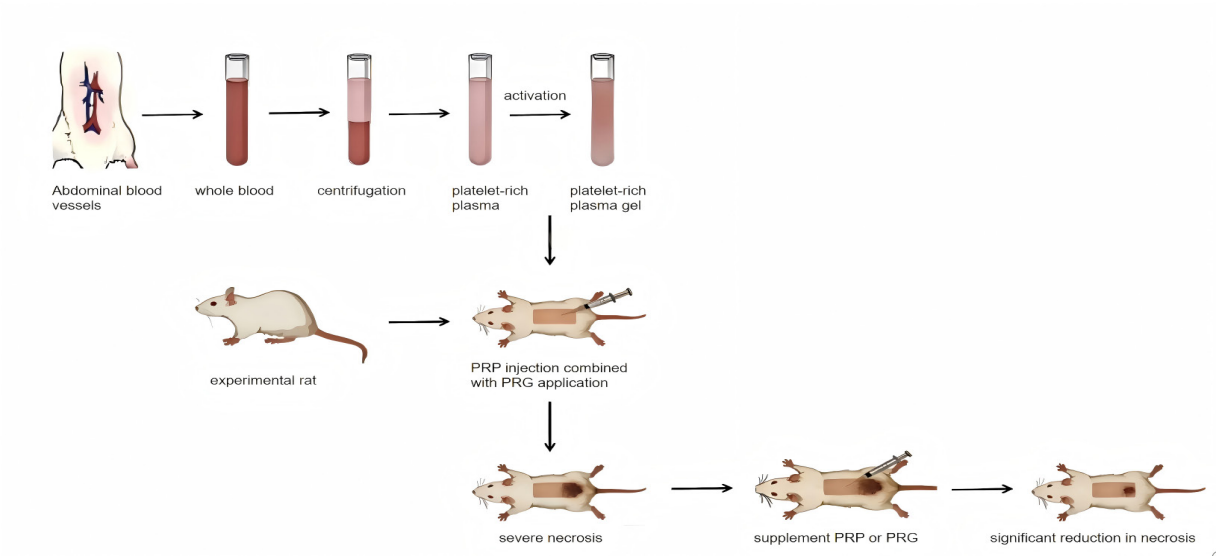

https://doi.org/10.71321/0x94xp56

The Mechanism of Platelet-Rich Plasma Added to Skin Flap Postoperative for the Influence of Skin Flap Survival

Chengyang Dong [1] , Zean Lin [1] , Linsen Fang [2*]

Received: 2025-12-17 | Accepted: 2026-04-14 | Published online: 2026-05-16

Abstract

Background: This study investigated the effects of postoperative platelet-rich plasma (PRP) supplementation on skin flap survival in a rat model.
Methods: A random-pattern skin flap model was established in rats. During surgery, PRP injection combined with platelet-rich gel (PRG) application was performed. On postoperative day 3, PRP or PRG was supplemented into the flap via uniform point injections. Necrotic area was recorded at postoperative day 7. Flap defect length and terminal edema severity were assessed by contrast-enhanced ultrasonography. Tissue specimens were collected for histopathological and immunohistochemical analysis. Relative expression levels of vascular endothelial growth factor (VEGF), platelet-derived growth factor (PDGF), and cluster of differentiation 34 (CD34) were measured.
Results: The group receiving intraoperative PRP injection combined with PRG application, followed by postoperative PRG supplementation, showed significantly shorter tissue defect lengths and less terminal tissue edema compared to other groups ($P<0.01$). Relative expression levels of VEGF, PDGF, and CD34 were significantly higher than those in other groups ($P<0.01$).
Conclusion: Postoperative PRP and PRG supplementation reduced flap defect length and edema severity, increased growth factor expression, and improved flap survival. PRG supplementation produced the most pronounced benefits.
Keywords: free flap; Platelet-Rich Plasma Gel; Platelet-Rich Plasma; ultrasound contrast; VEGF; CD34

Introduction

Skin flap transplantation is commonly used for reconstructing extensive burn wounds and deep injuries secondary to trauma or congenital defects. However, persistent issues such as delayed wound healing and incomplete recovery after flap surgery have been observed [1-2]. Research indicates that poor wound healing is associated with growth factor deficiency, as these factors play a crucial role in wound repair. Platelet-rich plasma (PRP) and platelet-rich gel (PRG), both platelet-rich blood products, contain activated platelets that release multiple growth factors including vascular endothelial growth factor (VEGF). These factors synergistically promote cell proliferation, migration, and angiogenesis, providing multiple positive effects in wound healing and serving as an effective adjunctive therapy to improve outcomes for difficult-to-heal wounds post-skin flap surgery [3-4]. However, partial necrosis may still occur after PRP-injected skin flaps. To investigate this, the research team developed a rat model of free flap. During surgery, 50μl/cm²PRP was injected and 50μl/cm²PRG was applied. Postoperatively, an additional 100μl/cm²PRP or PRG was administered. The study aimed to determine whether postoperative PRP supplementation could further increase growth factor levels, and enhance flap survival probability, thereby providing new insights for clinical PRP therapy in treating non-healing wounds.

Experimental Animals and Related Materials

Experimental Animals

86 healthy SPF-grade SD female rats (7-8 weeks old, 200-230g) were used in this study. 36 rats were allocated for experimental modeling, while 50 rats were used for PRP preparation. The rats were procured from the Experimental Animal Center of Anhui Medical University (License: SYXK (Wan) 2022-001) and maintained in a controlled environment with 20-28°C temperature and 45-75% humidity. Each cage contained four rats, with free access to food and water. The experiment was approved by the Anhui Medical University Laboratory Animal Ethics

1 Department of Burn, First Affiliated Hospital of Anhui Medical University, Hefei 230022, China
2 The First Affiliated Hospital of Anhui Medical University / Anhui Provincial Public Health Clinical Center Wound Repair and Plastic Surgery, Hefei 230012, China
* Corresponding Author.

Committee (Approval No.: LLSC20252051).

Main Reagents and Instruments

80°C ultra-low temperature freezer, DW-HL5 purchased from Zhongke Meiling Low-Temperature Technology; Excellent Low-Speed Benchtop Centrifuge, L3-5K purchased from Hunan Kecheng Instrument Equipment Co., Ltd.; Ultrasound Diagnostic Instrument, ACUSON Sequoia purchased from Siemens Medical Systems Co., Ltd.; Ruiwode Enhanced Small Animal Anesthesia Machine, R540 purchased from Shenzhen Ruiwode Life Technology Co., Ltd.; Fully Automatic Blood Cell Analyzer, BC-5390 CRP purchased from Mindray Medical International Co., Ltd.; High-Resolution Biological Microscope, DP74 purchased from Olympus. PDGF Antibody Reagents purchased from Hefei Shanben Biotechnology. VEGF antibodies were procured from Affinity; CD34 antibodies from Protein Tech; calcium gluconate injection from Sichuan Meidakanghua Pharmaceutical Co., Ltd.; and sulfur hexafluoride microbubbles for injections from Bracco Suisse SA.

PRP and PRG Preparation

Two female SD rats were randomly selected from 50 SD rats. The anesthetized rats were placed on the experimental table in supine position, and their limbs were fixed. The abdominal area was fully exposed, and the skin was cut along the white line of the abdomen to expose the abdominal vein. The blood was collected by a blood needle and 5ml of whole blood was taken. The whole blood was placed in 10% sodium citrate anticoagulation tube.

The whole blood was centrifuged at 200g for 20 minutes, and the whole blood was divided into red blood cell layer, white blood cell layer and plasma layer. Plasma and leukocyte layer were collected using a 1ml syringe, followed by a second 200g centrifugation for 10 minutes. The supernatant (top 3/4) was discarded, and the remaining 1/4 was homogenized to obtain plasma-rich plasma (PRP). Mix 1000 U of thrombin lyophilized powder with 1mL of 10% calcium gluconate injection to prepare the activator. Then, mix PRP with the activator in a 10:1 ratio to obtain PRG. The gel-like PRG is left undisturbed for 10-20 minutes until liquefaction, after which filtration yields the liquefied PRG.

Collect 0.1ml of platelet-rich plasma in a sterile EP tube and perform platelet count using the BC-5390 CRP blood cell analyzer. Ensure strict aseptic techniques throughout the procedure to prevent contamination.

Experimental Grouping

The experiment was divided into two parts: one group received 0.5ml saline injection in the flap during operation, and the other group received 0.25mlPRP injection in the flap combined with 0.25mlPRG application. After operation, the two parts received 0.5ml saline, 0.5mlPRP and 0.5mlPRG respectively. Rats were randomly divided into six groups: N+N, N+P, N+G, PG+N, PG+P, and PG+G.

Model Design Concept

The dorsal skin of rats exhibits abundant blood supply, primarily supplied by three arterial regions: the intercostal artery and lumbar artery in the central zone, the deep ilio-rotator artery in the lateral zone, and the thoracodorsal artery in the scapular zone [5]. Our preliminary experiments demonstrated that, given rats 'rich subcutaneous vascular supply and strong repair capacity, even retaining a single thoracodorsal artery as the primary donor would result in minimal necrotic area at the flap's distal end postoperatively. Therefore, this study proposes a free flap model where major vessels are severed intraoperatively, leaving only the dermis, subdermis, and microvascular network in the subcutaneous tissue for blood supply. This design increases the distal necrotic area of the flap, facilitating postoperative evaluation of PRP's therapeutic effects.

Skin Preparation

Place the rats in a small animal anesthesia machine. After inducing anesthesia with 3.0% isoflurane for 3 minutes, adjust the isoflurane concentration to 2.0%. Position the anesthetized rats prone on the experimental table. Use a small razor to remove back hair, then apply an experimental animal depilatory agent to eliminate residual hair roots. After thorough depilation, wipe off the depilatory agent with povidone-iodine to avoid skin burns.

Flap Design and Procedure

A 1×5cm rectangular skin flap was designed on the back of the rats, with the scapula as the pedicle. After routine disinfection and draping, the rat's skin and superficial fascia were incised along the marked line. The superficial fascia was dissected from the deep fascia using a tissue dissection scissors, and the flap was lifted in its entirety. The three major arteries supplying the flap were ligated to ensure the free flap was obtained. Following complete hemostasis, 50μl/cm² of PRP injection and 50μl/cm² of PRG application were performed at the flap base. The flap was then sutured in situ with 5-0 sutures, re-disinfected, and kept warm. Upon recovery, the rats were housed individually in cages to prevent mutual tearing.

Postoperative Addition of PRP or PRG

On the third postoperative day, anesthetized rats were placed prone on the experimental platform. Photographs were taken to record the necrotic area of the skin flap, which was then analyzed using Image Pro Plus software to calculate the necrotic area. After routine disinfection and draping, 0.5 ml of PRP was drawn with a 1ml syringe and uniformly injected as a spot at 1-2 mm from the flap edge. The other treatment group received the same dose of liquid PRG, while the control group received the same dose of saline. After anesthesia recovery, the rats were returned to their cages and continued under standard feeding conditions.

Ultrasound Contrast

Imaging and Flap Sampling On the seventh postoperative day, rats were anesthetized again and photographed to document necrotic flap area. The images were analyzed using Image Pro Plus software to calculate necrotic area. Rats were positioned supine on the experimental table, routinely disinfected, and gauze was laid. One side of the jugular vein was isolated and punctured with a cannula, which was then sutured (see figure below). A 0.5ml dose of sulfur hexafluoride microbubble contrast agent was injected uniformly via the cannula, followed by ultrasound contrast imaging guided by 10MHz ultrasound. Under contrast imaging, the length of the visual defect and the thickness of edema at the flap margin were recorded. A small amount of whole blood was taken for platelet count before eu-

thanizing the rats for sampling. The samples were processed separately for pathological immunohistochemistry.

Immunohistochemistry

The mouse skin samples were embedded in paraffin to prepare white slides for HE staining and immunohistochemical detection. HE staining was used to observe the gross morphology of tissues and infiltration extent of inflammatory markers in sections. Immunohistochemical staining was employed to detect the relative expression levels of VEGF and PDGF in tissues. Five randomly selected 400x field observations from each well-processed slide were scored, with the final score calculated as the average of five evaluations. Positive results were defined as brown-yellow or brown-brown staining particles localized to cytoplasm or cell membranes, with the percentage of positive cells counted as a percentage of skin tissue cells. Scoring criteria were as follows: 1) Staining: No staining = 0 points; light yellow = 1 point; light brown = 2 points; brown-brown = 3 points. 2) Positive cell percentage: 0% = 0 points; 1%–24% = 1 point; 25%–49% = 2 points; 50%–74% = 3 points; 75%–100% = 4 points. 3) The final score was determined by multiplying staining intensity by the percentage of positive cells. Statistical analysis was performed on the final scores of each group.

Microvessel Counting

Under the CD34 immunostaining field magnified 400 times, 5 non-adjacent areas were randomly selected for scoring. The number of microvessels was counted and averaged to determine the vascular density of each sample. Statistical analysis was performed on the microvessel counts of rats in each group.

Statistical Methods

Statistical analysis was performed using SPSS software. Quantitative data conforming to normal distribution were presented as mean ± standard deviation ($\bar{X}$±s). One-way ANOVA was employed for inter-group comparisons. For pairwise comparisons with homogeneous variances, the Bonferroni method was used. A P-value <0.05 was considered statistically significant.

Results

Platelet Count Analysis

Through statistical analysis of platelet counts in whole blood, intraoperative PRP, and postoperative PRP from all groups: The platelet count in whole blood of all groups was (622.53±52.70)×10^9 /L, with no significant intergroup differences (F=1.128; P=0.367). The platelet count in intraoperative PRP was (2469.50±225.75)×10^9 /L, which was 3.966 times that of whole blood, with no significant intergroup difference (F=2.479; P=0.139). The platelet count in postoperative PRP was (2287.81±168.65)×10^9 /L, which was 3.674 times that of whole blood, with no significant intergroup difference (F=2.409; P=0.118). (Table 1)

Contrast-enhanced Ultrasound

On the seventh postoperative day, contrast-enhanced ultrasound revealed no significant differences in normal tissue thickness among all rat groups in this study (**P**>0.05). Measurements of defect length and terminal edema in skin flaps showed that the PG+G group exhibited the smallest defect length and lightest terminal edema compared to other groups (**P**<0.05)(Figure 1). Compared with the N+N group, the N+P and N+G groups demonstrated significantly reduced terminal edema and defect severity (**P**<0.001). In contrast, the PG+N group exhibited more pronounced terminal edema and defect severity than the PG+P group (**P**<0.001), while the PG+G group showed marked improvement (**P**<0.05).

Flap Necrosis St atus

On the third postoperative day, all rat groups exhibited varying degrees of necrosis in the distal flap areas (Table 2). The PRP-treated group showed significantly reduced necrotic area compared to the saline-treated group (**P**<0.05). By the seventh day, the PG+P and PG+G groups demonstrated statistically significant reduction in necrotic area (**P**<0.001) compared to other groups. Notably, the N+P and N+G groups showed marked necrosis reduction (**P**<0.001) relative to the N+N group, while the PG+P and PG+G groups also exhibited decreased necrotic area (**P**<0.001) compared to the PG+N group. However, no significant difference was observed between PG+P and PG+G groups (**P**>0.05), nor between N+P and N+G groups (**P**>0.05). These results indicate that the saline-treated group showed further expansion of necrotic area by the seventh day, whereas

Table 1. Platelet count in whole blood and PRP of rats in each group ($\bar{X}$±s, 10^9/L)

Group	Number	whole blood	Intraoperative PRP	Postoperative PRP
N+N	6	—	—	—
N+P	6	613.33±26.80	—	2443.75±187.45
N+G	6	613.33±38.28	—	2307.25±157.86
PG+N	6	655.33±51.86	2425.50±113.66	—
PG+P	6	637.50±59.00	2644.50±30.23	2197.25±160.10
PG+G	6	622.50±49.68	2338.50±254.98	2203.81±55.43
F		1.128	2.479	2.409
P		0.367	0.139	0.118

Note: Data are expressed as mean ± standard deviation ($\bar{x}$±s), and one-way analysis of variance was performed. Bonferroni method was used for inter-group comparisons in this dataset. Statistical analysis showed no significant differences in platelet counts among the groups in whole blood, intraoperative PRP, and postoperative additional PRP. And PRP was not used at the horizontal line.

the PRP or PRG-treated groups maintained stable necrotic extent compared to the third-day baseline.

HE Staining

From HE staining of rat skin flaps postoperatively in all groups showed chronic inflammatory cell infiltration and epidermal shedding in all flap tissues. The N+N group exhibited the most pronounced inflammatory cell infiltration and epidermal shedding compared to other treatment groups(Figure 2A). In contrast, PG+G and PG+P groups demonstrated significantly fewer inflammatory cells and reduced epidermal shedding, with well-preserved epithelial cells(Figure 2E-F).

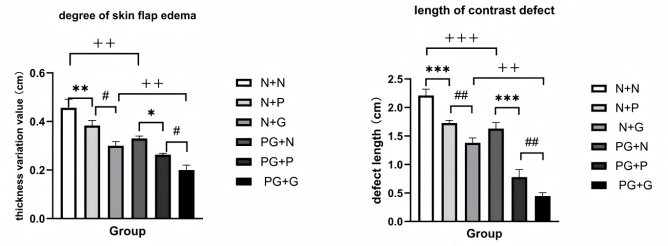

Figure 1. Comparison of flap edema degree and defect length on POD 7.
Comparison of flap edema severity and defect length on postoperative day 7 in six groups of rats. Thirty-six rats were randomly divided into a saline group (n=18, treated with normal saline) and an experimental group (n=18, treated with PRP+PRG). On postoperative day 3, the rats were further subdivided into three groups: an additional saline group (n=6), an additional PRP group (n=6), and an additional PRG group (n=6).On postoperative day 7, flap edema severity and defect length were measured using contrast-enhanced ultrasound. Data were presented as mean ± standard deviation (SD). Statistical analysis was performed using One-way ANOVA.

Note: *P<0.05 when comparing the additional PRP group; **P<0.01; ***P<0.001; #P<0.05 when comparing with the additional PRG group; #P<0.01; #P<0.001; +P<0.05 when comparing with the group receiving PRP combined with PRG during surgery, ++P<0.01; +++P<0.001. X-axis: Group N+N; Group N+P;Group N+G; Group PG+N; Group PG+P; Group PG+G. Y-axis: edema thickness of skin flap(cm); length of contrast defect(cm).

Table 2. The necrotic area of skin flaps ($\bar{X}$±s, cm^2)

Group	Number	D3	D7
N+N	6	3.37±0.27	4.01±0.19
N+P	6	3.31±0.19	3.34±0.17 [2]
N+G	6	3.39±0.29	3.28±0.16 [2,3]
PG+N	6	1.14±0.13 [5]	2.68±0.26 [2]
PG+P	6	1.57±0.19 [5]	1.60±0.17 [1,2]
PG+G	6	1.31±0.24 [5]	1.34±0.25 [1,2,4]
F		131.479	166.698
P		<0.001	<0.001

Note: Data are expressed as mean ± standard deviation ($\bar{x}$±s), and one-way analysis of variance was performed. Bonferroni method was used for inter-group comparisons in this dataset. 1 indicates P<0.001 compared to PG+N group; 2 indicates P<0.001 compared to N+N group; 3 indicates P>0.05 compared to N+P group; 4 indicates P>0.05 compared to PG+P group; 5 indicates P<0.05 compared to N+N, N+P, and N+G groups.

Immunohistochemical Analysis

On the seventh postoperative day, immunohistochemical analysis was performed on the rat skin flap specimens to detect the levels of growth factors including VEGF and PDGF. Results showed that: Compared with the N+N group, all other treatment groups exhibited significantly increased expression levels of PDGF and VEGF (**P**<0.05). Among the treatment groups with significant differences from the N+N group, the PG+G group demonstrated notably higher expression levels of PDGF and VEGF compared to other groups (**P**<0.05)(Figure 3, 4, and 5). Compared with the group receiving PRP postoperatively, all PRG groups showed marked increases in growth factor levels. Specifically, the N+G group exhibited significantly higher expression levels than the N+P group (**P**<0.05). The PG+G group showed significantly higher growth factor expression levels compared to the PG+P group, while the PG+N group showed significantly lower levels than the PG+P group (**P**<0.05) (Table 3).

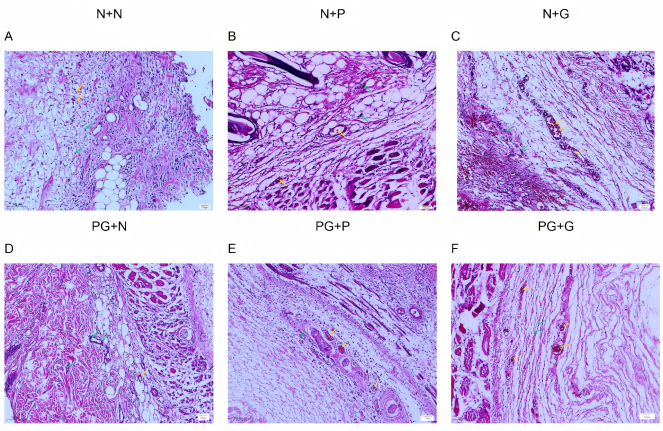

Figure 2. HE staining of rat skin flaps.
HE staining was performed to observe the integrity of tissue sections, the extent of inflammatory cell infiltration, and the number of blood vessels. HE staining revealed randomly selected sections. In group N+N, extensive inflammatory cell infiltration, vascular congestion, and tissue necrosis were observed. Group N+P with added PRP and Group N+G with added PRG showed better preservation of cell morphology and an increased number of blood vessels. Compared to group PG+N and group PG+P, group PG+G exhibited better tissue morphology, milder inflammatory infiltration, and a higher number of blood vessels. Yellow arrows indicate blood vessels; Green arrows indicate inflammatory cell infiltration. Scale =100 μm. HE staining: Hematoxylin-eosin staining.

Microvessel Count Analysis

Microvessel counts were determined through CD34 detection. Compared with other groups, the PG+G group showed a significantly higher number of microvessels (**P**<0.001). All other treatment groups exhibited statistically significant increases in microvessel count compared to the N+N group (**P**<0.05)(Figure 6-7). The N+G group demonstrated a significantly higher microvessel count than the N+P group (**P**<0.05), while the PG+P group showed a markedly higher count than the PG+N group (**P**<0.01)(Table 4).

Discussion

A random flap is a localized skin flap primarily supplied by the dermal

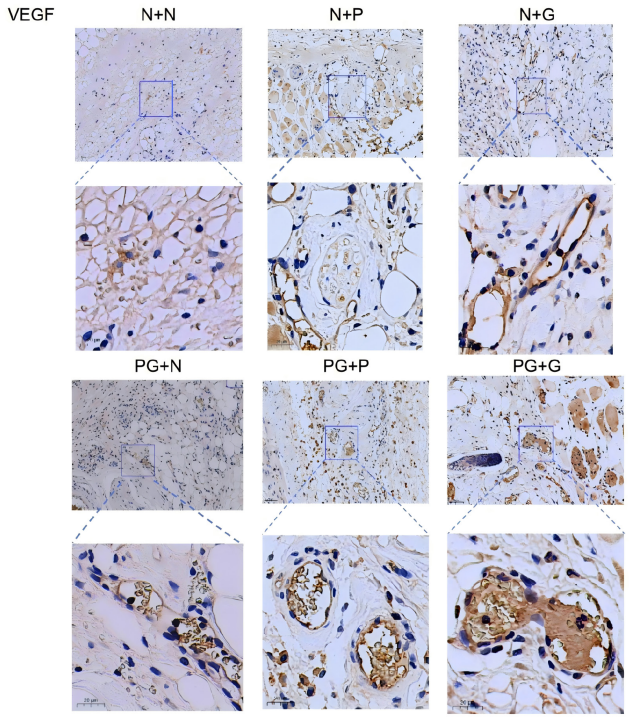

Figure 3. VEGF staining results

The relative expression levels of VEGF in tissues were detected by immunohistochemical staining. Five randomly selected sections with satisfactory staining were scored, and the final score was calculated as the average of the five scores. Positive results were defined as brown-yellow or brown-brown staining granules localized on the cytoplasm or cell membrane. The group receiving additional PRP or PRG showed a higher proportion of brownish-yellow areas and a higher final score. The group receiving saline supplementation exhibited a lower proportion of light yellow area scores. Scale = 20 μm.

layer, subdermal layer, and microvascular network within subcutaneous tissue, excluding dominant axial cardiovascular structures or large-caliber arteries with accompanying veins [6]. Due to unstable blood supply and limited perfusion range, the distal portion of such flaps is prone to ischemic necrosis [7]. Historically, it was believed that maintaining fixed length-to-width ratios was essential for achieving high flap survival rates. However, with advancements in anatomy, Milton et al. designed flaps with varying length-to-width ratios on pig backs—though all sharing the same blood supply base—revealing that flap survival depends not on specific ratios but on the underlying vascular supply [8]. This groundbreaking conclusion challenged the rigid constraints of fixed length-to-width ratios in random flaps. Rat dorsal skin is primarily supplied by three parallel vascular networks: the central region, fed by the posterior perforating branches of the intercostal and lumbar arteries, serves as the primary blood supply source; the lateral region is supplied by the deep ilio-rotator artery; and the scapular region by the thoracolumbar artery [5].This three-zone vascular "map" provides an anatomical basis for experimental design of random flaps. Additionally, the necrotic areas in rat flaps remain stable and can be precisely quantified using Image Pro Plus to calculate necrosis percentages, ensuring objective and reliable data. Based on these principles, the research team developed a rat model for random flap experiments, surgically isolating the axial cardiovascular structures within the region while preserving only the dermal layer and subcutaneous microvascular network to induce distal necrosis, with necrosis areas analyzed using Image Pro Plus software.

The essence of skin flap healing lies in establishing new blood supply and completing tissue repair under ischemic conditions. In the early postoperative period, the flap's blood supply is entirely dependent on the pedicle. Flaps distant from the pedicle experience ischemia and hypoxia due to inadequate blood perfusion, leading to lactic acid accumulation, cellular acidosis, reduced ATP production, and insufficient cellular energy supply [9]. As platelets aggregate and activate, temporary stromal formation releases inflammatory factors, initiating the inflammatory response. Excessive neutrophil activation, oxygen free radical bursts, tissue edema, and microthrombus formation cause ischemia-reperfusion injury, further exacerbating flap necrosis [10]. Around the third postoperative day, under the regulation of hypoxia-inducible factor-1α (HIF-1α), endothelial cells of the original blood vessels in the flap are activated by growth factors including vascular endothelial growth factor (VEGF), platelet-derived growth factor (PDGF).These cells proliferate and migrate to form new capillary buds, interconnecting to create a functional microvascular network that generates fresh blood supply to promote flap healing [10-11].

Platelet-rich plasma (PRP), a platelet-concentrated biological agent isolated through gradient centrifugation from autologous whole blood, contains platelets 3-5 times more abundant than peripheral blood. Platelet-rich gel (PRG), a gelatinous substance produced by adding activators to PRP, shares the ability to enhance growth factor concentrations and reduce inflammatory cytokine responses [12-

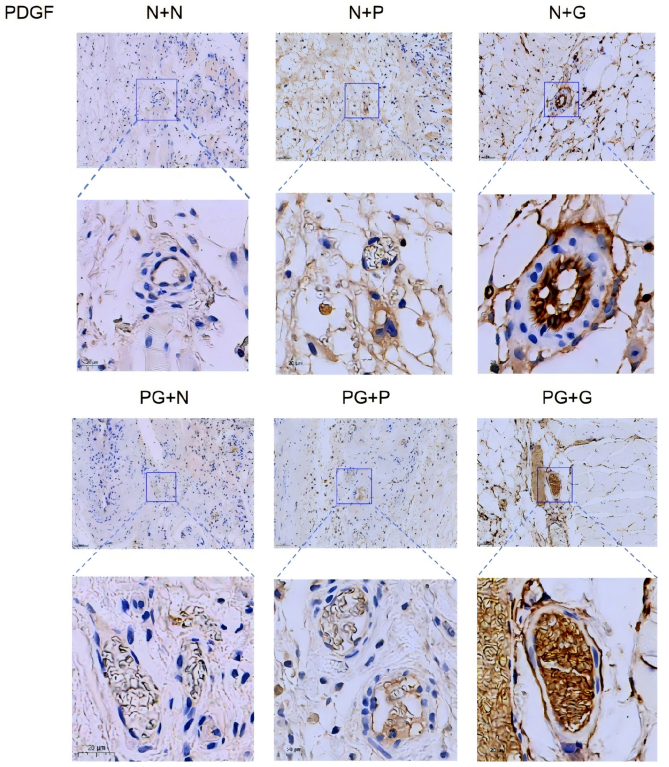

Figure 4. PDGF staining results.

The relative expression levels of PDGF in tissues were detected by immunohistochemical staining. Five randomly selected sections with satisfactory staining were scored, and the final score was calculated as the average of the five scores. Positive results were defined as brown-yellow or brown-brown staining granules localized on the cytoplasm or cell membrane. The group receiving additional PRP or PRG showed a higher proportion of brownish-yellow areas and a higher final score. Scale = 20 μm.

13]. However, due to the weight limitations of rats, autologous blood supply could not be achieved. This study therefore used allogeneic rat blood for PRP and PRG preparation. No significant immune rejection was observed during the experiment, consistent with Akbarzadeh S et al.'s findings [14]. Beyond its high platelet concentration, PRP contains multiple key growth factors, particularly platelet-derived growth factor (PDGF), vascular endothelial growth factor (VEGF). ELISA confirmed that these factors in PRP are 3-4 times higher than in ordinary plasma while maintaining high activity.

VEGF, a 45-kD heparin-binding dimeric glycoprotein, is recognized as the most potent regulator in angiogenesis induction [15]. By binding to its receptor VEGFR2, VEGF activates the P13K/AKT signaling pathway, which phosphorylates and activates endothelial nitric oxide synthase (eNOS) in endothelial cells. This increases NO production, thereby inducing vasodilation, promoting angiogenesis, and improving vascular permeability [16]. Kryger Z, Vourtsis SA et al. created rat skin flaps and administered VEGF suspension to the distal 1/3 flap through various delivery methods [17-18]. They found that under conditions of hypoxia and endothelial cell damage, regardless of delivery method, VEGF could enhance blood flow and flap survival in rat skin flaps. In our study, Point injections of PRP or PRG were administered at the flap margins, with photographic documentation followed by Image Pro Plus analysis of necrotic areas. The analysis of the data revealed that the saline group showed significantly increased necrotic area by day 7 compared to day 3. In contrast, the PRP or PRG groups demonstrated no significant difference in necrotic extent between days 3 and 7. These findings suggest that while PRP supplementation cannot reverse necrotic outcomes, it effectively delays the progression of necrosis. Immunohistochemical analysis further demonstrated markedly higher growth factor levels in PRP/PRG groups compared to saline control, with PRG supplementation showing more substantial improvements. The results indicate that PRP/PRG supplementation enhances tissue growth factor concentrations, activates vascular endothelial cells to promote angiogenesis, and delays necrotic progression, thereby improving necrosis rates. However, these effects were limited in flaps already showing significant necrosis.

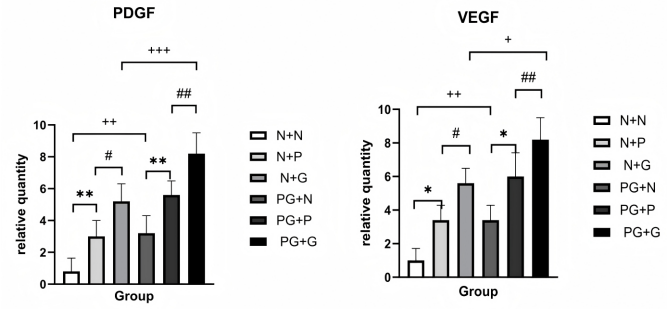

Figure 5. Relative expression levels of VEGF and PDGF

The relative expression levels of VEGF and PDGF in tissues were detected by immunohistochemical staining. Five randomly selected sections with satisfactory staining were scored, and the final score was calculated as the average of the five scores. Positive results were defined as brown-yellow or brown-brown staining granules localized on the cytoplasm or cell membrane. Data were presented as mean ± standard deviation (SD). Statistical analysis was performed using One-way ANOVA. *P<0.05 when comparing the additional PRP group ; **P<0.01; ***P<0.001; #P<0.05 when comparing with the additional PRG group; #P<0.01; #P<0.001; +P<0.05 when comparing with the group receiving PRP combined with PRG during surgery,++P<0.01; +++P<0.001. X-axis: Group N+N; Group N+P; Group N+G; Group PG+N; Group PG+P; Group PG+G. Y-axis: relative quantity.

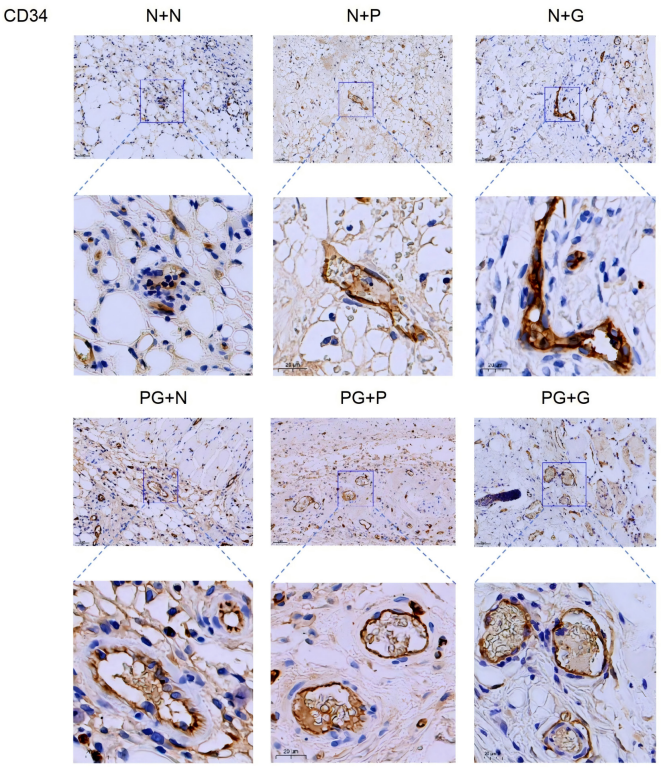

Figure 6. CD34 staining results.

Under the background of CD34 staining, 5 non-adjacent areas were randomly selected for scoring. The number of microvessels was counted and averaged to determine the vascular density of each sample. The stained sections revealed that the group supplemented with PRP and PRG exhibited a higher number of microvessels.

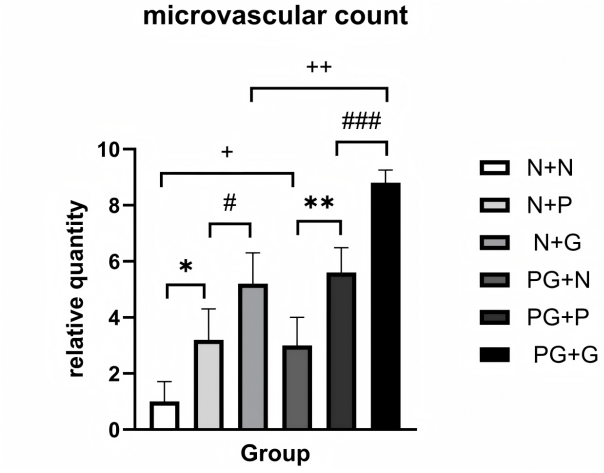

Figure 7. Microvessel Counting

Microvessel density (MVD) was expressed as the number of CD34-positive vessels per high-power field under light microscopy, with 5 randomly selected fields counted per slide. Data were presented as mean ± standard deviation (SD). Statistical analysis was performed using One-way ANOVA.*P<0.05 when comparing the additional PRP group ; **P<0.01; ***P<0.001; #P<0.05 when comparing with the additional PRG group; #P<0.01; #P<0.001; +P<0.05 when comparing with the group receiving PRP combined with PRG during surgery.++P<0.01; +++P<0.001. X-axis: Group N+N; Group N+P; Group N+G; Group PG+N; Group PG+P; Group PG+G. Y-axis:relative quantity.

Table 3. Statistical table of immunohistochemical results ($\bar{X}$±s).

Group	Number	PDGF			VEGF		
		Intensity	Percentage	Total	Intensity	Percentage	Total
N+N	6	0.60±0.89	0.40±0.55	0.80±0.84	0.80±0.45	1.00±0.71	1.00±0.71
N+P	6	1.60±0.55	2.00±0.45	3.00±1.00 [2]	1.60±0.55	2.20±0.45	3.40±0.89 [2]
N+G	6	2.40±0.55	2.20±0.45	5.20±1.10 [3,5]	2.20±0.45	2.60±0.55	5.60±0.89 [3,5]
PG+N	6	1.80±0.45	1.80±0.45	3.2±1.10 [2]	1.60±0.55	2.20±0.45	3.40±0.89 [2]
PG+P	6	2.20±0.45	2.60±0.55	5.60±0.89 [4,5]	2.20±0.45	2.80±0.84	6.00±1.41 [4,5]
PG+G	6	2.80±0.45	3.00±0.71	8.20±1.30 [1,4,5]	2.80±0.45	3.00±0.71	8.20±1.30 [1,4,5]
F				29.867			28.873
P				<0.001			<0.001

Note: Data are expressed as mean ± standard deviation ($\bar{x}$±s), and one-way analysis of variance was performed. Bonferroni method was used for inter-group comparisons in this dataset. 1 indicates P<0.05 compared to PG+P group; 2 indicates **P**<0.05 compared to N+N group; 3 indicates **P**<0.05 compared to N+P group; 4 indicates **P**<0.05 compared to PG+N group; 5 indicates **P**<0.001 compared to N+N group.

Table 4. Statistical table of microvascular count results($\bar{X}$±s)

Group	Number	Microvascular Count
N+N	6	1.00±0.71
N+P	6	3.20±1.10 [2]
N+PG	6	5.20±1.10 [1,3]
PG+N	6	3.00±1.00 [2]
PG+P	6	5.60±0.89 [1,4]
PG+PG	6	8.80±0.45 [1,5]
F		44.539
P		<0.001

Note: Data are expressed as mean ± standard deviation ($\bar{x}$±s), and one-way analysis of variance was performed. Bonferroni method was used for inter-group comparisons. 1 indicates **P**<0.001 compared to N+N group; 2 indicates **P**<0.05 compared to N+N group; 3 indicates **P**<0.05 compared to N+P group; 4 indicates **P**<0.01 compared to PG+N group; 5 indicates **P**<0.001 compared to PG+P group.

Ischemic necrosis of rat skin flaps typically manifests as characteristic blackening, crusting, hardened texture, and absence of blood flow upon needle puncture at the distal flap. While these macroscopic signs may initially suggest vascular impairment, they fail to accurately reflect the pathological and physiological state of subcutaneous tissues. Epidermal appearance often fails to correlate with the extent of subcutaneous edema or the defect range in microcirculatory perfusion imaging. Contrast-enhanced ultrasonography (CEUS) utilizes contrast agents such as sulfur hexafluoride microbubbles, with their diameter strictly controlled within 2-5μm. These microbubbles are completely metabolized through respiratory pathways within 15 minutes, eliminating dependence on hepatic and renal metabolic systems. Data from a large-scale multicenter clinical study involving 460,000 patients demonstrated an adverse event rate of merely 0.034%, with severe allergic reactions occurring at an even lower rate of 0.001% highlighting CEUS' advantages of high stability, excellent imaging quality, low diffusion, high biocompatibility, and safety [19-21]. In this study, CEUS revealed that compared to the group receiving only saline postoperatively, the group receiving PRP showed significantly smaller imaging defects and milder edema. Notably, the PG+G group demonstrated the best results, with both the length of imaging defects and flap edema being significantly lower than other treatment groups.

Conclusion

The findings demonstrate that postoperative application of platelet-rich plasma (PRP) or platelet-rich gel (PRG) significantly improves subcutaneous tissue defect coverage and reduces flap edema. By elevating growth factor concentrations (eg: VEGF), these treatments enhance vascular regeneration in recipient sites, thereby improving flap survival rates and delaying necrosis. Notably, PRG exhibits superior efficacy. This study provides novel therapeutic strategies for reducing postoperative necrosis and accelerating wound healing in clinical flap transplantation.

Abbreviations

Colony Differentiation Antigen 34: CD34; Vascular Endothelial Growth Factor: VEGF; Platelet-Derived Growth Factor: PDGF; Platelet-Rich Plasma Gel:PRG; Platelet-Rich Plasma : PRP; Nitric Oxide:NO; Vascular Endothelial Growth Factor Receptor 2: VEGFR2; Contrast-Enhanced Ultrasound: CEUS; Hypoxia-Inducible Factor-1α: HIF-1α.

Author Contributions

Linsen Fang: Conceptualization, Methodology, Resources, Supervision, Project administration, Funding acquisition. Chengyang Dong: Conceptualization, Methodology, Software, Validation, Formal analysis, Investigation, Data curation, Writing - Original Draft, Writing - Review & Editing, Visualization. Zean Lin: Investigation. Writing - Original Draft. All authors read and approved the final manuscript.

Acknowledgements

Not Applicable.

Funding Information

Clinical Medicine Peak Discipline Construction Project of Anhui Medical University (Grant No. 9301001815).

Ethics Approval and Consent to Participate

Not Applicable.

Competing Interests

The authors declare that they have no existing or potential commercial or financial relationships that could create a conflict of interest at the time of conducting this study.

Data Availability

All data needed to evaluate the conclusions in the paper are present in the paper or the Supplementary Materials. Additional data related to this paper may be requested from the authors.

References

[1] Ershadifar, S., Colback, A., Basmaci, U. N., Wilson, M., Birkeland, A. C., and Silverman, D. A. Predictors of Donor-Site Wound Complications Following Fibula Free Flap Reconstruction. OTO Open. 2025;9(2):e70126. https://doi.org/10.1002/oto2.70126

[2] Yang, J., Qin, X., Hou, L., and Liu, Y. Risk prediction models for complications after flap repair surgery: a systematic review and meta-analysis. BMC Surgery. 2025;25(1):398. https://doi.org/10.1186/s12893-025-03072-8

[3] Marx, R. E. Platelet-rich plasma: evidence to support its use. Journal of Oral and Maxillofacial Surgery. 2004;62(4):489–496. https://doi.org/10.1016/j.joms.2003.12.003

[4] Everts, P., Onishi, K., Jayaram, P., Lana, J. F., and Mautner, K. Platelet-Rich Plasma: New Performance Understandings and Therapeutic Considerations in 2020. International Journal of Molecular Sciences. 2020;21(20):7794. https://doi.org/10.3390/ijms21207794

[5] Yang, D., and Morris, S. F. Comparison of two different delay procedures in a rat skin flap model. Plastic and Reconstructive Surgery. 1998;102(5):1591–1597. https://doi.org/10.1097/00006534-199810000-00039

[6] Zhang, D., Jin, C., Han, T., Chen, J., Ali Raza, M., Li, B., et al. Sinomenine promotes flap survival by upregulating eNOS and eNOS-mediated autophagy via PI3K/AKT pathway. International Immunopharmacology. 2023;116:109752. https://doi.org/10.1016/j.intimp.2023.109752

[7] Harder, Y., Amon, M., Erni, D., and Menger, M. D. Evolution of ischemic tissue injury in a random pattern flap: a new mouse model using intravital microscopy. Journal of Surgical Research. 2004;121(2):197–205. https://doi.org/10.1016/j.jss.2004.03.026

[8] Milton, S. H. Pedicled skin-flaps: the fallacy of the length: width ratio. British Journal of Surgery. 1970;57(7):502–508. https://doi.org/10.1002/bjs.1800570705

[9] Lee, J. H., You, H. J., Lee, T. Y., and Kang, H. J. Current Status of Experimental Animal Skin Flap Models: Ischemic Preconditioning and Molecular Factors. International Journal of Molecular Sciences. 2022;23(9):5234. https://doi.org/10.3390/ijms23095234

[10] Landén, N. X., Li, D., and Ståhle, M. Transition from inflammation to proliferation: a critical step during wound healing. Cellular and Molecular Life Sciences. 2016;73(20):3861–3885. https://doi.org/10.1007/s00018-016-2268-0

[11] Eming, S. A., Martin, P., and Tomic-Canic, M. Wound repair and regeneration: mechanisms, signaling, and translation. Science Translational Medicine. 2014;6(265):265sr6. https://doi.org/10.1126/scitranslmed.3009337

[12] Collins, T., Alexander, D., and Barkatali, B. Platelet-rich plasma: a narrative review. EFORT Open Reviews. 2021;6(4):225–235. https://doi.org/10.1302/2058-5241.6.200017

[13] Boswell, S. G., Cole, B. J., Sundman, E. A., Karas, V., and Fortier, L. A. Platelet-rich plasma: a milieu of bioactive factors. Arthroscopy. 2012;28(3):429–439. https://doi.org/10.1016/j.arthro.2011.10.018

[14] Akbarzadeh, S., McKenzie, M. B., Rahman, M. M., and Cleland, H. Allogeneic Platelet-Rich Plasma: Is It Safe and Effective for Wound Repair? European Surgical Research. 2021;62(1):1–9. https://doi.org/10.1159/000514223

[15] Ferrara, N., and Kerbel, R. S. Angiogenesis as a therapeutic target. Nature. 2005;438(7070):967–974. https://doi.org/10.1038/nature04483

[16] Carmeliet, P., and Jain, R. K. Molecular mechanisms and clinical applications of angiogenesis. Nature. 2011;473(7347):298–307. https://doi.org/10.1038/nature10144

[17] Vourtsis, S. A., Spyriounis, P. K., Agrogiannis, G. D., Ionac, M., and Papalois, A. E. VEGF application on rat skin flap survival. Journal of Investigative Surgery. 2012;25(1):14–19. https://doi.org/10.3109/08941939.2011.593693

[18] Kryger, Z., Zhang, F., Dogan, T., Cheng, C., Lineaweaver, W. C., and Buncke, H. J. The effects of VEGF on survival of a random flap in the rat: examination of various routes of administration. British Journal of Plastic Surgery. 2000;53(3):234–239. https://doi.org/10.1054/bjps.1999.3315

[19] Shang, Y., Xie, X., Luo, Y., Nie, F., Luo, Y., Jing, X., et al. Safety findings after intravenous administration of sulfur hexafluoride microbubbles to 463,434 examinations at 24 centers. European Radiology. 2023;33(2):988–995. https://doi.org/10.1007/s00330-022-09108-4

[20] Newsome, I. G., and Dayton, P. A. Acoustic Angiography: Superharmonic Contrast-Enhanced Ultrasound Imaging for Noninvasive Visualization of Microvasculature. Methods in Molecular Biology. 2022;2393:641–655. https://doi.org/10.1007/978-1-0716-1803-5_34

[21] Lv, K., Zhai, H., Jiang, Y., Liang, P., Xu, H. X., Du, L., et al. Prospective assessment of diagnostic efficacy and safety of SonazoidTM and SonoVue® ultrasound contrast agents in patients with focal liver lesions. Abdominal Radiology. 2021;46(10):4647–4659. https://doi.org/10.1007/s00261-021-03010-1